Mathematical modeling in scheduling cancer treatment with combination of VEGF inhibitor and chemotherapy drugs

Xiulan Lai, Avner Friedman

PII: S0022-5193(18)30571-X
DOI: https://doi.org/10.1016/j.jtbi.2018.11.018
Reference: YJTBI 9720

To appear in: *Journal of Theoretical Biology*

Received date: 26 February 2018
Revised date: 15 November 2018
Accepted date: 19 November 2018

Please cite this article as: Xiulan Lai, Avner Friedman, Mathematical modeling in scheduling cancer treatment with combination of VEGF inhibitor and chemotherapy drugs, *Journal of Theoretical Biology* (2018), doi: https://doi.org/10.1016/j.jtbi.2018.11.018

Highlights

- A mathematical model is developed to describe the interactions between two anticancer drugs in the treatment of metastatic breast cancer.
- Since one of the drugs (anti-VEGF) is antagonistic to the other (chemotherapy drug), we address the question how to schedule the treatment in order to reduce antagonism and increase treatment efficacy.
- In contrast with common approach to administer the two drugs at the same time, we show that administering the two drugs non-overlappingly yields significant better benefits.

Mathematical modeling in scheduling cancer treatment with combination of VEGF inhibitor and chemotherapy drugs

Xiulan Lai[a], Avner Friedman[b,*]

[a] *Institute for Mathematical Sciences, Renmin University of China, Beijing, P. R. China*
[b] *Mathematical Bioscience Institute & Department of Mathematics, Ohio State University, Columbus, OH, USA*

Abstract

The present paper considers a treatment of cancer with a combination of anti-VEGF (bevacizumab) and a chemotherapy drug (docetaxel). Since anti-VEGF reduces the perfusion of chemotherapy drugs, the question arises whether it is more effective to administer the two drugs at the same time, or non-overlapping, in order to reduce tumor volume more effectively. To address this question we develop a mathematical model and use it to simulate different schedules. We find that the treatment of cancer would be far more effective if the two drugs are given non-overlappingly, with the chemotherapy drug at day 0 and anti-VEGF at day 7 in cycles of 21 days.

Keywords: Combination therapy, anti-VEGF, chemotherapy, scheduling, mathematical model
2010 MSC: 00-01, 99-00

1. Introduction

Chemotherapy is a treatment given to slow or stop the growth of cancer by killing cancer cells, and it is given in cycles. A cycle is the time between two administrations of the drug; this time is needed to allow the body to recover from the side effects of the medicine. A typical cycle of chemotherapy is 21 or 28 days.

In clinical trials in metastatic breast cancer with combination of chemotherapy drug and anti-VEGF, reported in [1, 2, 3, 4, 5, 6, 7], the two drugs are administered at the same time in each cycle. Since anti-VEGF reduces the perfusion of chemotherapy drugs [8, 9, 10, 11], the question arises whether it would be more beneficial to inject the two drugs non-overlappingly instead of at the

*Corresponding author
Email address: afriedman@math.osu.edu (Avner Friedman)

same time. Recent mice experiments show that, indeed, this will be more reduction in tumor volume when the two drugs are administered non-overlappingly [12], as was also suggested by a PK/PD model [12].

In clinical trials with combination therapy it is often the case that not sufficient forethought is given to the interaction between the diverse agents [13], and this may contribute to the failure of many phase III clinical trials [14]. In the case of metastatic breast cancer there have been clinical trials with combination of a chemotherapy drug and anti-VEGF where the two drugs are administered at the same time in each cycle. But anti-VEGF adversely affects the effectiveness of the chemotherapy, since it reduces the perfusion of chemotherapy drugs . Hence, the question arises whether it would be more beneficial to inject the two drugs non-overlappingly instead of at the same time. Recent mice experiments show that, indeed, there will be more reduction in tumor volume growth when the two drugs are administered non-overlappingly [12], as was also suggested by a PK/PD model .

In the present paper we develop a mathematical model of combination therapy for caner with anti-VEGF (e.g. bevacizumab, sunitinib) and chemotherapy (e.g. docetaxel, paclitaxel) and use the model to compare two schedules: simultaneous injections and successive (non-overlapping) injections. The model is represented by a system of partial differential equations (PDEs) with the following variables: densities of cancer cells, dendritic cells, $CD8^+$ T cells and endothelial cells, and concentrations of IL-12, VEGF, oxygen, and the two drugs. The model is based on the network shown in Fig. 1. As depicted in this figure, cancer immunogenicity activates dendritic cells, who then activate $CD8^+$ T cells, by IL-12, and the activated T cells kill cancer cells. VEGF secreted by cancer cells attracts endothelial cells into the tumor, initiating a process of angiogenesis, which brings oxygen to the cancer cells. VEGF also blocks maturation of dendritic cells and of $CD8^+$ T cells. Fig. 1 shows also the effect of two drugs.

We measure the effectiveness of a treatment by how many days it takes to reduce the initial tumor volume by 98%. Simulations of the model show that non-overlapping injections of the two drugs, with the chemotherapy administered at day 0 and anti-VEGF at day 7, or vice versa, in cycles of 21 days, is much more effective than injecting both drugs at the same time, in the same cycle of 21 days.

2. Mathematical model

The mathematical model is based on Fig. 1. The list of variables is given in Table 1.

Radiological images of tumors show heterogeneity and plasticity, but for simplicity we assume that the total density of cells within the tumor is constant, which does not change in time:

$$D + T_8 + E + C = \text{constant}. \tag{1}$$

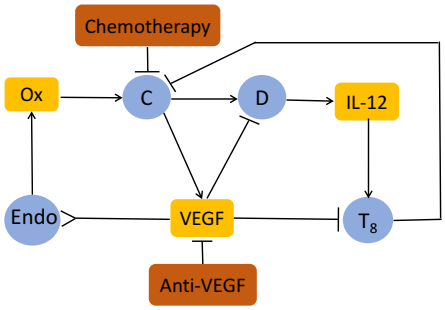

Figure 1: **Interaction of immune cells with cancer cells**. Sharp arrows indicate proliferation/activation, blocked arrows indicate killing/blocking, and the inverted arrow indicates recruitment/chemoattraction. C: cancer cells, D: dentritic cells, T_8: $CD8^+$ T cells, Endo: endothelial cells, Ox: Oxygen from the blood.

Table 1: List of variables (in unit of g/cm^3).

Notation	Description
D	density of Dendritic cells (DCs)
T_8	density of activated $CD8^+$ T cells
E	density of Endothelial cells
C	density of cancer cells
I_{12}	IL-12 concentration
W	oxygen concentration
G	VEGF concentration
A	chemotherapy drug concentration
B	anti-VEGF concentration

We also assume that the densities of debris of dead cancer cells, of immature dendritic cells, and of naive $CD8^+$ T cells remain constant throughout the tumor tissue. Under the assumption (1), proliferation of cancer cells and immigration of endothelial cells and $CD8^+$ T cells into the tumor, give rise to internal pressure which results in cells movement. We assume that all the cells move with the same velocity, $\mathbf{u}$; $\mathbf{u}$ depends on space and time and will be taken in unit of cm/day. We assume that all the cytokines and anti-tumor drugs are diffusing within the tumor, and that also all the cells undergo dispersion (i.e. diffusion).

Equation for DCs (D). By necrotic cancer cells we mean cancer cells undergoing the process of necrosis. Necrotic cancer cells release HMGB-1 [15]. We model the dynamics of the necrotic cells (N_C) and HMGB-1 (H) by the

following equations:

$$\frac{\partial N_C}{\partial t} + \underbrace{\nabla\cdot(\mathbf{u}N_C)}_{\text{velocity}} - \underbrace{\delta_{N_C}\nabla^2 N_C}_{\text{difusion}} = \underbrace{\lambda_{N_C C} C}_{\text{derived from life cancer cells}} - \underbrace{d_{N_C} N_C}_{\text{removal}},$$

$$\frac{\partial H}{\partial t} - \underbrace{\delta_H \nabla^2 H}_{\text{difusion}} = \underbrace{\lambda_{HN_C} N_C}_{\text{released from nerotic cancer cells}} - \underbrace{d_H H}_{\text{degradation}},$$

where $\lambda_{N_C C}$ is the rate at which cancer cells become necrotic and λ_{HN_C} is the rate at which necrotic cells produce HMGB-1. We note that since molecules are several orders of magnitude smaller than cells, they are only marginally influenced by the cells velocity $\mathbf{u}$, so their velocity may be neglected. The degradation of HMGB-1 is fast ($\sim$0.01/day) [16], and we assume that the removal process of necrotic cells is also fast. We may then approximate the two dynamical equations by the steady state equations $\lambda_{N_C C} C - d_{N_C} N_C = 0$ and $\lambda_{HN_C} N_C - d_H H = 0$, so that H is then proportional to C.

Dendritic cells are activated by HMGB-1 [17, 18]. Hence, the activation rate of immature dendritic cells, with density D_0, is proportional to $D_0 \frac{H}{K_H + H}$, or to $D_0 \frac{C}{K_C + C}$, since H is proportional to C. Here, the Michaelis-Menten law was used to account for the limited rate of receptor recycling time which takes place in the process of DCs activation. The dynamics of DCs is then given by

$$\frac{\partial D}{\partial t} + \underbrace{\nabla\cdot(\mathbf{u}D)}_{\text{velocity}} - \underbrace{\delta_D \nabla^2 D}_{\text{difusion}} = \underbrace{\lambda_{DC} D_0 \frac{C}{K_C + C}}_{\text{activation by HMGB-1}} \cdot \underbrace{\frac{1}{1 + G/K_{DG}}}_{\text{inhibition by VEGF}} \cdot \underbrace{(1 + \varepsilon_{DA} A)}_{\text{enhancement by } A} - \underbrace{d_D D}_{\text{death}}, \tag{2}$$

where δ_D is the diffusion coefficient, d_D is the death rate of DCs, and $1/(1 + G/K_{DG})$ represents the impairment of maturation of dendritic cells by VEGF [19, 20]. Chemotherapy induces immunogenic cell death that makes dying cells present more antigens to DCs. Thus the DC-activation term should include the contribution of cancer cells dying from the chemotherapy drug. We assume that the density of these dying cells is proportional to the concentration A of the chemotherapy drug, and represent the corresponding increase in the DC-activation by the factor $(1 + \varepsilon_{DA} A)$.

Equation of CD8^+ T cells (T_8). Inactive CD8^+ T cells are activated by IL-12 [21, 22], a process resisted by VEGF [23, 24, 25, 26, 27]. Hence,

$$\frac{\partial T_8}{\partial t} + \nabla\cdot(\mathbf{u}T_8) - \delta_T \nabla^2 T_8 = \underbrace{\lambda_{T_8 I_{12}} T_{80} \cdot \frac{I_{12}}{K_{I_{12}} + I_{12}}}_{\text{activation by IL-12}} \cdot \underbrace{\frac{1}{1 + G/K_{TG}}}_{\text{inhibition by VEGF}} - \underbrace{d_{T_8} T_8}_{\text{death}}, \tag{3}$$

where T_{80} is the density of the inactive CD8^+ T cells.

Equation for endothelial cells (E). Endothelial cells are chemoattracted by VEGF, and their proliferation is increased by VEGF [28, 29]. The equation

for the density of endothelial cells is given by

$$\frac{\partial E}{\partial t} + \nabla \cdot (\mathbf{u}E) - \delta_E \nabla^2 E = \underbrace{\lambda_E(G)E\left(1 - \frac{E}{E_M}\right)}_{\text{proliferation}} - \underbrace{\nabla \cdot (\chi_G E \nabla G)}_{\text{recruited by VEGF}} - \underbrace{d_E E}_{\text{death}}, \tag{4}$$

where E_M is the carrying capacity of endothelial cells, $\lambda_E(G) = \lambda_{EG}(G - G_0)^+$, and G_0 is a threshold below which the proliferation of E does not occur [30].

Equation for cancer cells (C). We assume a logistic growth for cancer cells with carrying capacity (C_M) in order to account for competition for space among these cells. The proliferation rate depends on the density of oxygen (W) [29]. The chemotherapy drug (e.g. docetaxel), A, kills cancer cells during the cell cycle. This is represented by reducing the proliferation rate of C by a factor $\mu_{CA}A$. But since anti-VEGF reduces perfusion of A, we need to replace A by $\frac{A}{1+B/K_{AB}}$. Hence the equation for C takes the form:

$$\begin{aligned}\frac{\partial C}{\partial t} + \nabla \cdot (\mathbf{u}C) - \delta_C \nabla^2 C = &\underbrace{\lambda_C(W)C\left(1 - \frac{C}{C_M}\right)}_{\text{proliferation}} \cdot \left(1 - \mu_{CA}A \cdot \frac{1}{1 + B/K_{AB}}\right) \\ &- \underbrace{\eta_8 T_8 C}_{\text{killing by T cells}} - \underbrace{d_C C}_{\text{death}},\end{aligned} \tag{5}$$

where η_8 is the killing rate of cancer cells by $CD8^+$ T cells, and d_C is the natural death rate of cancer cells. We take

$$\lambda_C(W) = \begin{cases} \lambda_{CW}\frac{W}{W_0} & \text{if } W \le W_0 \\ \lambda_{CW} & \text{if } W > W_0, \end{cases}$$

where W_0 is the normal oxygen concentration.

Equation for IL-12 (I_{12}). The proinflammatory cytokine IL-12 is secreted by activated DCs [21, 22], so that

$$\frac{\partial I_{12}}{\partial t} - \delta_{I_{12}} \nabla^2 I_{12} = \underbrace{\lambda_{I_{12}D} D}_{\text{production by DCs}} - \underbrace{d_{I_{12}} I_{12}}_{\text{degradation}}. \tag{6}$$

Equation for oxygen (W). Oxygen is infused through blood [28, 29]. We identify the blood concentration with the density of endothelial cells, and accordingly, write the equation for W in the following form:

$$\frac{\partial W}{\partial t} - \delta_W \nabla^2 W = \underbrace{\lambda_{WE} E}_{\text{source from blood}} - \underbrace{d_W W}_{\text{consumption by cells}}, \tag{7}$$

where $d_W W$ represents the take-up rate of oxygen by all the cells.

Equation for VEGF (G). VEGF is produced by cancer cells [28, 29]. Anti-VEGF treatment down-regulates VEGF. Hence the equation for G is given by

$$\frac{\partial G}{\partial t} - \delta_G \nabla^2 G = \underbrace{\lambda_G(W)C}_{\text{production by cancer cells}} - \underbrace{\mu_{GB}GB}_{\text{inhibition by anti-VEGF}} - \underbrace{d_G G}_{\text{degradation}} \quad (8)$$

where B is the anti-VEGF concentration in the tumor. Here, we assume, as in [31] that the secretion rate of VEGF by cancer cells is at its maximum level when W is at a certain hypoxic level W^*, but it decreases when W increases above W^* or when W decreases below W^*, and take

$$\lambda_G(W) = \lambda_{GW} \times \begin{cases} \frac{W}{W^*} & \text{if } 0 \le W \le W^* \\ 1 - 0.7\frac{W-W^*}{W_0-W^*} & \text{if } W^* < W \le W_0 \\ 0.3 & \text{if } W > W_0. \end{cases}$$

Equation for chemotherapy (A). We denote by γ_A the effective level of the injected chemotherapy drug A during the dosing period, and by μ_{AC} the depletion rate of A through killing of cancer cells. Hence,

$$\frac{\partial A}{\partial t} - \delta_A \nabla^2 A = \gamma_A I_A(t) - \underbrace{\mu_{AC}CA}_{\text{depletion through killing cancer}} - \underbrace{d_A A}_{\text{degradation}}, \quad (9)$$

where $I_A(t) = \sum_{j=1}^{n} \gamma_A \mathrm{e}^{-\alpha(t-t_i^A)} H(t-t_i^A)$ and $H(t) = 1$ if $t < 0$, and $H(t) = 0$ if $t > 0$; the drug is injected at days t_j^A.

Equation for anti-VEGF (B). We denote by γ_B the effective level of the injected anti-VEGF drug (B) during the dosing period, and by μ_{BG} the depletion rate of B while blocking VEGF. The equation for B is given by

$$\frac{\partial B}{\partial t} - \delta_B \nabla^2 B = \gamma_B I_B(t) - \underbrace{\mu_{BG}GB}_{\text{depletion by VEGF}} - \underbrace{d_B B}_{\text{degradation}}, \quad (10)$$

where $I_B(t) = \sum_{j=1}^{m} \gamma_B \mathrm{e}^{-\alpha(t-t_i^B)} H(t-t_i^B)$; the drug is injected at days t_j^B.

Equation for cells velocity (u). We take the steady state density of endothelial cells to be $E = 2.5 \times 10^{-3}$ g/cm^3 [30]. As estimated in the section of parameter estimation, the average steady state densities of the immune cells D, T_8, and C are taken to be (in unit g/cm^3)

$$D = 4 \times 10^{-4}, \quad T_8 = 1 \times 10^{-3}, \quad C = 0.4. \quad (11)$$

To be consistent with Eq. (1) we take the constant on the RHS of Eq. (1) to be 0.4039. We further assume that all cells have approximately the same diffusion coefficient. Adding Eqs. (2)-(5), we get

$$0.4039 \times \nabla \cdot \mathbf{u} = \sum_{j=2}^{5} [\text{right-hand side of Eq. (j)}]. \quad (12)$$

To simplify the computations, we assume that the tumor is spherical and denote its radius by $r = R(t)$. We also assume that all the densities and concentrations are radially symmetric, that is, they are functions of (r, t), where $0 \le r \le R(t)$. In particular, $\mathbf{u} = u(r,t)\mathbf{e}_r$, where $\mathbf{e}_r$ is the unit radial vector.

Equation for free boundary (R). We assume that the free boundary $r = R(t)$ moves with the velocity of cells, so that

$$\frac{dR(t)}{dt} = u(R(t), t). \tag{13}$$

Boundary conditions We assume that inactive $CD8^+$ T cells that migrated from the lymph nodes into the tumor microenvironment have constant density $\hat{T}_8$ at the tumor boundary, and, upon entering the boundary, that T_8 are activated by IL-12. We then have the following flux condition at the tumor's boundary:

$$\frac{\partial T_8}{\partial r} + \sigma_T(I_{12})(T_8 - \hat{T}_8) = 0, \quad \text{at } r = R(t), \tag{14}$$

where we take $\sigma_T(I_{12}) = \sigma_0 \frac{I_{12}}{I_{12}+K_{I_{12}}}$. We assume that the endothelial cells which are attracted by VEGF into the tumor microenvironment have constant densities $\hat{E}$ at the tumor boundary, so that

$$\frac{\partial E}{\partial r} + \sigma_E \frac{G}{K_G + G}(E - \hat{E}) = 0, \quad \text{at } r = R(t). \tag{15}$$

We also assume

$$\text{no-flux for } D, C, I_{12}, W, G, A, \text{ and } B \text{ at } r = R(t). \tag{16}$$

Initial conditions We take the following initial values (in units g/cm^3):

$$\begin{aligned} &D = 2 \times 10^{-3},\ T_8 = 2 \times 10^{-3},\ E = 2.45 \times 10^{-3},\ C = 0.39565, \\ &I_{12} = 2.88 \times 10^{-9},\ W = 1.52 \times 10^{-4},\ G = 6.3 \times 10^{-8},\ R(0) = 0.01 \text{ cm}. \end{aligned} \tag{17}$$

Note that the total density of cells satisfies Eq. (1) with the chosen constant 0.4039. We also note that the somewhat arbitrary choice of initial conditions does not affect the simulation results after a few days.

3. Results

The simulations of the model were performed by Matlab based on the moving mesh method for solving partial differential equations with free boundary [32] (see the section on computational method).

Figure 2 shows the average densities of cells and cytokines for the first 30 days, and the growth of tumor volume. We see that the level of oxygen in the first few days varies aound W^* ($W^* = 1.69 \times 10^{-4}$ g/cm^3, by Table 3), which

affects the growth rate of C as well as the production rate of G by C, resulting in initial oscillation of G, after which G begins to increase. The increase in G results in a decrease in D, I_{12} and T_8, and the decrease in T_8 results in an increase in C. We also see that the tumor volume increases from 4.19×10^{-6} cm^3 to 2.7×10^{-4} cm^3 in 30 days. We note that each species X tends to a steady state which is approximately the half-saturation value K_X that was assumed in estimating some of the model parameters. This shows a consistency in the parameters estimation.

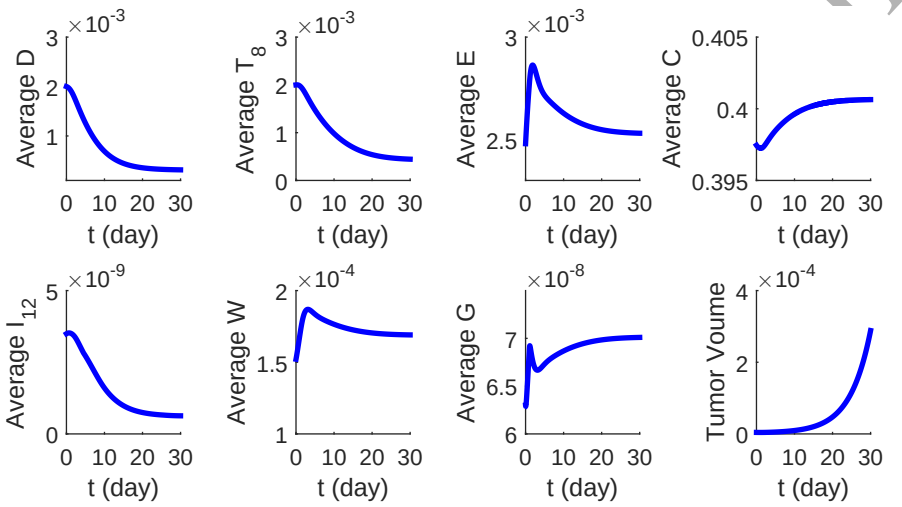

Figure 2: Average densities/concentrations, in g/cm^3, of all the variables of the model in control case (no drugs). All parameter values are the same as in Tables 2 and 3, for a mouse model.

Proceeding as in mice experiments, we apply the anti-VEGF and chemotherapy drug and observe the effect of these agents, separately and in combination, on the growth of the tumor volume. We note that, in our model, the amounts γ_B and γ_A are proportional to the dose amounts injected into the mice, but these two proportionality coefficients are not known. We view γ_B and γ_A as the "effective" dose amounts, and we determine their order of magnitude by comparing the simulations of the tumor volume growth with experimental results [33, 34, 35] in mice models for breast cancer.

Recall that we model the functions $I_A(t)$ and $I_B(t)$ in Eqs. (9) and (10) as follows:

$$I_A(t) = \gamma_A \sum_{t_j^A < t} e^{-\alpha_A (t - t_j^A)}, \quad I_B(t) = \gamma_B \sum_{t_j^B < t} e^{-\alpha_B (t - t_j^B)}.$$

where t_j^A and t_j^B are the days at which the drugs A and B, respectively, were injected; t_j^A and t_j^B are increasing with respect to j. The parameters γ_A, α_A and γ_B, α_B will be adjusted for each of the three experiments in [33], [34] and [35];

however, for illustration, we take $\alpha_A = \alpha_B = 5$/day, and, accordingly, adjust γ_A and γ_B, but other choices of α_A, α_B can be taken with corresponding changes in γ_A, γ_B.

In the schedule used in [33] both drugs were given twice a week for 3 weeks, so that $t_j^A = t_j^B$ vary over the days 3,7,10,14,18,21,24,28. Using this schedule, Fig. 3(a) shows the profiles of the tumor volumes with $\gamma_B = 6\times10^{-9}$ g/cm$^3\cdot$day and $\gamma_A = 3 \times 10^{-9}$ g/cm$^3 \cdot$ day. We see that the chemotherapy drug reduced the tumor volume more than anti-VEGF, and the combination of the two drugs reduced the tumor volume more than each drug alone; this is in agreement with the results reported in [33].

In the schedule used in [34] anti-VEGF was given 3 times in the first week, followed by chemotherapy 3 times a week for two weeks, so that $t_j^B = 1, 3, 5$ and $t_j^A = 8, 10, 12, 15, 17, 19$. Taking $\gamma_B = 9 \times 10^{-9}$ g/cm$^3 \cdot$ day and $\gamma_A = 5 \times 10^{-9}$ g/cm$^3 \cdot$ day, Fig. 3(b) shows profiles similar to Fig. 3(a), and it is in agreement with the results reported in [34].

We next consider the schedule used in [35] with anti-VEGF is given twice a week for 3 weeks, that is, at days $t_j^B = 3, 7, 10, 14, 17, 21, 24, 28, 31, 35, 38, 42$, and the chemotherapy is given once every 3 weeks, that is, at days $t_j^A = 10, 31$. Using this schedule with $\gamma_B = 2.1 \times 10^{-8}$ g/cm$^3 \cdot$ day and $\gamma_A = 1.2 \times 10^{-8}$ g/cm$^3 \cdot$ day, Fig. 3(c) shows that anti-VEGF reduced the tumor volume more than the chemotherapy, in agreement with results reported in [35]. As in [35], Fig. 3(c) also shows that under the combination therapy the reduction in tumor volume decreases a little bit at day 10 and 31 when the chemotherapy is given, but when the chemotherapy is stopped, the reduction in tumor-volume increase is almost as the case when only the anti-VEGF is injected, in agreement with [35].

3.1. Scheduling of treatment

In clinical trials for cancer with combination therapy, the question how to schedule the injections of the two drugs should take into account the interaction that may take place between the diverse agents [36, 37, 38, 39]. In the present paper we consider the scheduling issue in the case of combination therapy of anti-VEGF (e.g. bevacizumab) and a chemotherapy drug (e.g. docetaxel).

In clinical trials the treatment and follow-up periods are much longer than in mouse models, and the tumor growth is slower. Accordingly we modify some parameters in order to slow the growth of the tumor; these parameters are λ_{CW}, λ_E, λ_{DC}. In mice experiments [33, 34, 35] the tumor volume is continuously increasing, but in clinical trials we expect the tumor volume to decrease. The range of γ_B and γ_A will be taken accordingly.

We consider three different schedules with cycle of 21 days. In the first schedule, S1, both drugs anti-VEGF and the chemotherapy are administered at the same time in the first week of each cycle; in the second schedule, S2, the chemotherapy is administered in the first week and anti-VEGF in the second week; and in the third schedule, S3, anti-VEGF is administered in the first

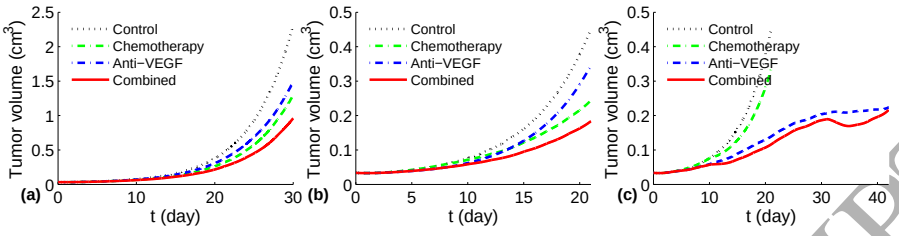

Figure 3: Growth of tumor volume under treatment with γ_B or γ_A, or combination (γ_B, γ_A). (a) Following the same schedule as in [33], both drugs were given twice a week for 3 weeks, that is, in days 3,7,10,14,21,24,28 with $\gamma_B = 6 \times 10^{-9}$ g/cm^3 · day and $\gamma_A = 3 \times 10^{-9}$ g/cm^3 · day. (b) Following the same schedule as in [34]: anti-VEGF was given 3 times in the first week, that is, at days $t_j^B = 1, 3, 5$, with $\gamma_B = 9 \times 10^{-9}$ g/cm^3 · day followed by chemotherapy 3 times a week for two weeks, that is, at days $t_j^A = 8, 10, 12, 15, 17, 19$, with $\gamma_A = 5 \times 10^{-9}$ g/cm^3 · day. (c) Following the same schedule as in [35], anti-VEGF is given twice a week, that is, at days $t_j^B = 3, 7, 10, 14, 17, 21, 24, 28, 31, 35, 38, 42$, with $\gamma_B = 2.1 \times 10^{-8}$ g/cm^3 · day, but the chemotherapy is given once every 3 weeks, that is, at days $t_j^A = 10, 31$, with $\gamma_A = 1.2 \times 10^{-8}$ g/cm^3 · day. $R(0) = 0.2$cm . All other parameter values are the same as in Tables 2 and 3, for a mouse model.

week, followed by the chemotherapy in the second week. We define the efficacy of a treatment by the time it takes to reduce the initial tumor volume by 98%. Figure 4 shows the efficacy of each of the three schedules. In this figure, the amounts of injected γ_B and γ_A are marked on the horizontal and vertical axes, respectively, and the efficacy, i.e., the time, in weeks, it took to reduce the tumor volume by 98%, it marked on the color columns. Figures 4(a), 4(b), 4(c) corresponds to schedules S1, S2 and S3, respectively. We see that under Schedule S1 (simultaneous injections of γ_B, γ_A), the efficacy ranges from 20 to 70 weeks, while under non-overlapping schedules S2 and S3 the efficacy ranges from 18 weeks to 42 weeks in Fig. 4(b), and from 13 weeks to 35 weeks in Fig. 4(c). We conclude that non-overlapping injections yield significantly better results than simultaneous injection of the two drugs. We also see that schedule S3 is somewhat more effective than schedule S2.

Simultaneous injection (S1) is significantly less effective than non-overlapping injections (S2, S3), because anti-VEGF blocks the perfusion of chemotherapy. Schedule S3 is somewhat more effective than schedule S2 for the following reason. Since chemotherapy kills directly cancer cells, when anti-VEGF is applied in schedule S2, there are already considerably less cancer cells, and hence the full power of the anti-VEGF drug is not realized. On the other hand, under schedule S3, the reduction in cancer cells under anti-VEGF is indirect, namely, through reduction in endothelial cells and oxygen (Eqs. (4), (7)), which take some time. Hence, the chemotherapy effectiveness is only slightly decreased by the preceding injection of anti-VEGF.

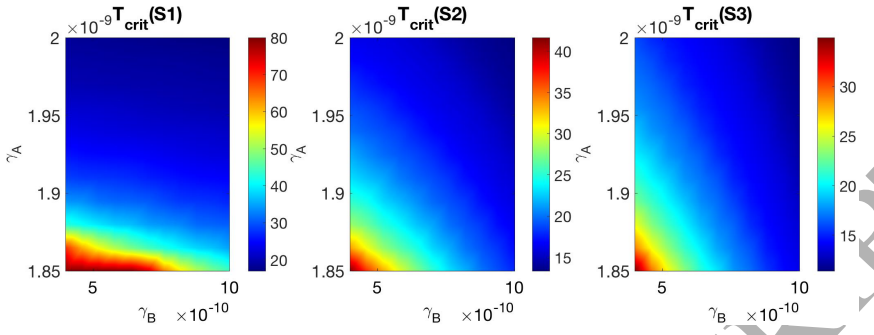

Figure 4: **Efficacy maps: The time in weeks (T_{crit}) at which the tumor volume decreases by 98% of its initial size under treatment** (γ_B, γ_A)**.** (A) Efficacy map under schedule S1, T_{crit}(S1); (B) Efficacy map under schedule S2, T_{crit}(S2); (C) Efficacy map under schedule S3, T_{crit}(S3). The color columns show how many weeks it took for the tumor volume to be reduced by 98%. All parameter values are the same as in Tables 2 and 3, for a human model.

4. Conclusion

Chemotherapy is administered intervenously in cycles of 21 days or 28 days in order to allow the body to recover from the side effects of the drug. Anti-VEGF (e.g. bevacizumab) is a common anticancer drug that blocks angiogenesis. Some treatments combine anti-VEGF with a chemotherapy drug (e.g. docetaxel), and both drugs were injected at the same time [1, 2]. Clinical trials with this combination therapy were reported in [3, 4, 5] (in cycles of 21 days) and in [6] (in cycle of 28 days). Since anti-VEGF reduces perfusion of chemotherapy in breast cancer [8, 9, 10, 11], one may ask whether it would be more effective, instead of injecting the two drugs at the same time (as in [1, 2, 3, 4, 5]) to inject the two drugs non-overlappingly, e.g., one drug in the first week and the second drug in the second week of a cycle. In the present paper we addressed this question by a mathematical model. The model includes cancer cells, dendritic cells, T cells, endothelial cells, IL-12 and oxygen. The interactions among these variables, and the two drugs, are represented by a system of PDEs. We used the model to simulate three different schedules: injecting the two drugs at the same time (schedule S1), injecting the chemotherapy first, at day 0, and anti-VEGF drug at day 7 (schedule S2), and reversing the order, with anti-VEGF followed by chemotherapy (schedule S3), in a cycle of 21 days. We quantified the effectiveness of a treatment by the number of weeks it takes to decrease the initial volume of the tumor by 98%. Our finding is that schedules S2 and S3 are far more effective than schedule S1, and S3 in slightly more effective than S2. These results, however, need to be confirmed experimentally and clinically.

The method and results of the present paper can be extended to other combination therapies, and could play a role in the design of future clinical trials.

Table 2: Summary of parameter values

Notation	Description	Value used	References
δ_D	diffusion coefficient of DCs	8.64×10^{-7} cm^2 day^{-1}	[40]
δ_T	diffusion coefficient of T cells	8.64×10^{-7} cm^2 day^{-1}	[40]
δ_E	diffusion coefficient of endothelial cells	8.64×10^{-7} cm^2 day^{-1}	[40]
δ_C	diffusion coefficient of tumor cells	8.64×10^{-7} cm^2 day^{-1}	[40]
$\delta_{I_{12}}$	diffusion coefficient of IL-12	6.05×10^{-2} cm^2 day^{-1}	[41]
δ_W	diffusion coefficient of oxygen	0.8 cm^2 day^{-1}	estimated
δ_G	diffusion coefficient of VEGF	8.64×10^{-2} cm^2 day^{-1}	[42]
δ_A	diffusion coefficient of chemotherapy drug	0.27 cm^2 day^{-1}	estimated
δ_B	diffusion coefficient of anit-VGEF	4.70×10^{-2} cm^2 day^{-1}	estimated
σ_T	flux rate of T_8 cells at the boundary	1 cm^{-1}	[40]
σ_E	flux rate of endocelial cells at the boundary	1 cm^{-1}	[40]
χ_G	chemoattraction coefficient of VEGF	10 cm^5/g $\cdot$ day	[43, 44]
λ_{DC}	activation rate of DCs by tumor cells (mice)	11 day^{-1}	estimated
λ_{DC}	activation rate of DCs by tumor cells (human)	6 day^{-1}	estimated
$\lambda_{T_8 I_{12}}$	activation rate of CD8$^+$ T cells by IL-12	2.25 day^{-1}	estimated
λ_{EG}	growth rate of endothelial cells (mice)	2.54×10^7 cm^3/g $\cdot$ day	estimated
λ_{EG}	growth rate of endothelial cells (human)	2.28×10^7 cm^3/g $\cdot$ day	estimated
λ_{CW}	growth rate of cancer cells (mice)	2.24 day^{-1}	estimated
λ_{CW}	growth rate of cancer cells (human)	1.92 day^{-1}	estimated
$\lambda_{I_{12}D}$	production rate of IL-12 by DCs	2.21×10^{-6} day^{-1}	[41]
λ_{WE}	production rate of oxygen by endothelial cells	7×10^{-2} day^{-1}	[30]
λ_{GW}	production rate of VEGF by cancer cells	2.21×10^{-6} day^{-1}	estimated

Appendix

Parameter estimation

Half-saturation

In an expression of the form $Y\frac{X}{K_X+X}$ where Y is activated by X, the parameter K_X is called the "half-saturation" of X. We assume that if the average density (or concentration) of X,

$$\frac{\int X dx}{\int X},$$

converges to a steady state X_0, then

$$\frac{X_0}{K_X + X_0}$$

is not "too small" and not "too close" to 1, and for definiteness we take

$$\frac{X_0}{K_X + X_0} = \frac{1}{2}$$

so that

$$K_X = X_0. \tag{18}$$

To estimate parameters, we assume that all the average densities and concentrations converge to steady states, and thus use Eq. (18) in each of the steady state equations of the model.

Table 3: Summary of parameter values

Notation	Description	Value used	References
d_D	death rate of DCs	0.1 day^{-1}	[40]
d_{T_8}	death rate of $CD8^+$ T cells	0.18 day^{-1}	[40]
d_E	death rate of endothelial cells	0.69 day^{-1}	[30]
d_C	death rate of tumor cells	0.17 day^{-1}	[40]
$d_{I_{12}}$	degradation rate of IL-12	1.38 day^{-1}	[40]
d_W	take-up rate of oxygen by cells	1.04 day^{-1}	estimated
d_G	degradation rate of VEGF	12.6 day^{-1}	[30]
d_A	degradation rate of anti-PD-L1	1.23 day^{-1}	estimated
d_B	degradation rate of anti-VEGF	0.17 day^{-1}	estimated
η_8	killing rate of cancer cells by T cells	120.75 $\text{cm}^3/\text{g}\cdot\text{day}$	estimated
μ_{CA}	blocking rate of cancer growth by chemotherapy	10^8 cm^3/g	estimated
μ_{AC}	degradation rate of chemotherapy by blocking cancer	27.68 $\text{cm}^3/\text{g}\cdot\text{day}$	estimated
μ_{GB}	degradation rate of VEGF by anti-VEGF	2.19×10^9 $\text{cm}^3/\text{g}\cdot\text{day}$	estimated
μ_{BG}	degradation rate of anti-VEGF in blocking VEGF	2.19×10^7 $\text{cm}^3/\text{g}\cdot\text{day}$	estimated
ε_{DA}	promotion rate of DCs by chemotherapy	10^8 cm^3/g	estimated
K_{DG}	blocking rate of maturation of DCs by VEGF	2.8×10^{-7} g/cm^3	estimated
K_{TG}	blocking rate of activation of T cells by VEGF	2.8×10^{-7} g/cm^3	estimated
K_{AB}	blocking perfusion rate of chemotherapy by anti-VEGF	10^{-9} g/cm^3	estimated
γ_A	injection rate of chemotherapy (in mice)	$0-1.2\times10^{-8}$ $\text{g/cm}^3\cdot\text{day}$	estimated
γ_B	injection rate of anti-VEGF (in mice)	$0-2.1\times10^{-8}$ $\text{g/cm}^3\cdot\text{day}$	estimated
γ_A	injection rate of chemotherapy (in human)	$0-2\times10^{-9}$ $\text{g/cm}^3\cdot\text{day}$	estimated
γ_B	injection rate of anti-VEGF (in human)	$0-12.1\times10^{-9}$ $\text{g/cm}^3\cdot\text{day}$	estimated
K_D	half-saturation of $CD4^+$ T cells	4×10^{-4} g/cm^3	[41]
K_{T_8}	half-saturation of $CD8^+$ T cells	1×10^{-3} g/cm^3	[41]
K_E	half-saturation of endothelial cells	2.5×10^{-3} g/cm^3	[30]
K_C	half-saturation of tumor cells	0.4 g/cm^3	[41]
$K_{I_{12}}$	half-saturation of IL-12	8×10^{-10} g/cm^3	[41]
K_W	half-saturation of oxygen	1.69×10^{-4} g/cm^3	[30]
K_G	half-saturation of VGEF	7×10^{-8} g/cm^3	[30]
D_0	density of immature DCs	2×10^{-5} g/cm^3	[40]
T_{80}	density of naive $CD8^+$ T cells	2×10^{-4} g/cm^3	[41]
E_M	carrying capacity of endothelial cells	5×10^{-3} g/cm^3	[30]
C_M	carrying capacity of cancer cells	0.8 g/cm^3	[40]
G_0	threshold VEGF concentration	3.65×10^{-10} g/cm^3	[30]
$\hat{T}_8$	density of $CD8^+$ T cells from lymph node	2×10^{-3} g/cm^3	[41]
$\hat{E}$	density of endothelial cells from outside of tumor	5×10^{-3} g/cm^3	[30]
W^*	hypoxia threshold oxygen level	1.69×10^{-4} g/cm^3	[31]
W_0	normal threshold oxygen level	4.65×10^{-4} g/cm^3	[31]

Diffusion coefficients

By [45], the diffusion coefficient δ_p and the molecular weight M_p of any protein p are related by the formula $\delta_p = \frac{\text{constant}}{M_p^{1/3}}$. Hence,

$$\delta_p = \frac{M_G^{1/3}}{M_p^{1/3}}\delta_G,$$

where M_G and δ_G are, respectively, the molecular weight and diffusion coefficient of VEGF; $M_G = 24$kDa [46] and $\delta_G = 8.64\times10^{-2}\ \text{cm}^2\,\text{day}^{-1}$ [42]. Since $M_{I_{12}} =$ 70kDa [47], $\delta_{I_{12}} = 6.05\times10^{-2}\ \text{cm}^2\ \text{day}^{-1}$. We apply this formula also to the drugs; since $M_B = 149$kDa (bevacizumab), we get $\delta_B = 4.70\times10^{-2}\ \text{cm}^2\,\text{day}^{-1}$;

since $M_A = 807.89$Da, we get $\delta_A = 0.27$ cm^2 day^{-1}. The diffusion coefficient of oxygen in the extracellular matrix (EMC) is in the range of $7 \times 10^{-6} - 2 \times 10^{-5}$ cm^2/s [48]; we take it to be $\delta_W = 0.8$cm^2/day.

Eq. (2).

From the steady state of Eq. (2), we get $\lambda_{DC} D_0 \frac{C}{K_C + C} \cdot \frac{1}{1+G/K_{DG}} = d_D D$, where, by [41], $d_D = 0.1$/day, $C = K_C = 0.4$ g/cm^3, $D = K_D = 4 \times 10^{-4}$ g/cm^3, $D_0 = 2 \times 10^{-5}$ g/cm^3. We assume that $K_{DG} = 4K_G$ where $K_G = 7 \times 10^{-8}$ g/cm^3 [30]; hence $\lambda_{DC} = 2.5 d_D D/D_0 = 5$/day.

In using the steady state equation, we ignored the fact that tumor volume is increasing, which causes a dilution in the average density. We need to compensate for this dilution by increasing the production term. We take $\lambda_{DC} = 11$/day in mice and $\lambda_{DC} = 6$/day in human. When chemotherapy drug is administered, we take $\varepsilon_{DA} = 10^8$ cm^3/g.

Eq. (3).

We assume that $K_{TG} = 4K_G$ where $K_G = 7 \times 10^{-8}$ g/cm^3 [30]. From the steady state of Eq. (3) (more precisely, by setting to zero the right-hand side of Eq. (3), we have

$$\lambda_{T_8 I_{12}} T_{80} \cdot \frac{1}{2} \cdot \frac{4}{5} - d_{T_8} T_8 = 0$$

where, by [41], $d_{T_8} = 0.18$/day, $T_{80} = 2 \times 10^{-4}$ g/cm^3, $T_8 = K_{T_8} = 1 \times 10^{-3}$ g/cm^3. Hence $\lambda_{T_8 I_{12}} = 2.25$/day.

Because of the dilution effect (as in the estimation of $\lambda_D C$), we need to increase $\lambda_{T_8 I_{12}}$. However, since the boundary condition for T_8 brings new cells into the tumor tissue which was ignored in the steady state equation, we need, at the same time, also to decrease $\lambda_{T_8 I_{12}}$. We assume that the two effects cancel each other, and keep $\lambda_{T_8 I_{12}} = 2.25$/day.

Eq. (4).

By [30], $d_E = 0.69$/day, $E_M = 5 \times 10^{-3}$ g/cm^3, $K_E = 2.5 \times 10^{-3}$ g/cm^3, $\hat{E} = 5 \times 10^{-3}$ g/cm^3, $G_0 = 3.65 \times 10^{-10}$. We take $E_M = 2K_E = 5 \times 10^{-3}$ g/cm^3. From the steady state of Eq. (4) (we may ignore the chemotactic term, since there is no-flux of G from the boundary), we get $\lambda_{EG} = 2d_E/(K_G - G_0) = 1.98 \times 10^7$ cm^3/g $\cdot$ day.

Here, as in the case of $\lambda_{T_8 I_{12}}$, we need to consider the effect on λ_{EG} due to dilution, but also the effect of the influx of endothelial cells stimulated by VEGF. We assume that the influx of endothelial cells is more dominant, and increase λ_{EG} by a factor 1.28 in mice, so that $\lambda_{EG} = 2.54 \times 10^7$ cm^3/g $\cdot$ day in mice. We take $\lambda_{EG} = 2.28 \times 10^7$ cm^3/g $\cdot$ day in human.

Eq. (5).

We take $d_C = 0.17$ day^{-1}, $C_M = 0.8$ g/cm^3 [40] and $\lambda_{CW} = 1.6$/day [49]. In the steady state of the control case (no anti-tumor drugs), we assume that C is approximately 0.4 g/cm^3, and $W = W_0 = K_W = 1.69 \times 10^{-4}$ g/cm^3 (see

the estimates of Eq. (7)). In the the control case, from the steady state of Eq. (5), we have

$$\frac{1}{2}\lambda_{CW}K_W/W_0 - \eta_8 K_{T_8} - d_C = 0,$$

where $K_{T_8} = 1 \times 10^{-3}$ g/cm^3; hence $\eta_8 = (\lambda_C K_W/(2W_0) - d_C)/K_{T_8} = 120.75$ cm^3/g $\cdot$ day. In the control case, including the effect of the advection term and the fact that the tumor grows, we need to increase the growth rate of cancer cells; we take $\lambda_{CW} = 2.24$/day in mice and $\lambda_{CW} = 1.92$/day in human. When chemotherapy drug and anti-VEGF are administered, we take $\mu_{CA} = 10^8$ cm^3/g, and $K_{AB} = 10^{-9}$ g/cm^3.

Eq. (7).

From steady state of Eq. (7), we get $\lambda_{WE}E - d_W W = 0$, where $\lambda_{WE} = 7 \times 10^{-2}$/day [30], $W = K_W = 1.69 \times 10^{-4}$ g/cm^3 [30], $E = K_E = 2.5 \times 10^{-3}$ g/cm^3. Hence, $d_W = \lambda_{WE}E/W = 1.04$/day. Note that since we have already included the dilution effect for E we do not include it in the equation for W.

Eq. (8).

From steady state of Eq. (8) we get $\lambda_{GW}C - d_G G = 0$, where $d_G = 12.6$/day [30], $G = K_G = 7 \times 10^{-8}$ g/cm^3 [30], $C = K_C = 0.4$ g/cm^3. Hence, $\lambda_{GW} = 2.21 \times 10^{-6}$/day.

Eqs. (9)-(10).

The half-life of docetaxel is 13.5 hours [50], so that $d_A = \frac{\ln 2}{13.5/24} = 1.23$ day^{-1}, and assume that 90% of A is used in blocking growth of cancer cells, while the remaining 10% degrades naturally. Hence, $\mu_{AC}CA/90\% = d_A A/10\%$, so that

$$\mu_{AC} = \frac{9d_A}{C} = \frac{9 \times 1.23}{0.4} = 27.68\,\text{cm}^3/\text{g} \cdot \text{day}.$$

By [51], the half-life of anti-VEGF is 2.82-4.58 days; we take it to be 4 days, so that $d_B = \frac{\ln 2}{4} = 0.17$ day^{-1}. We assume that 90% of B is used in blocking VEGF, while the remaining 10% degrades naturally. Hence, $\mu_{GB}GB/90\% = d_B B/10\%$, so that

$$\mu_{BG} = \frac{9d_B}{G} = \frac{9.17}{7 \times 10^{-8}} = 2.19 \times 10^7\,\text{cm}^3/\text{g} \cdot \text{day}.$$

We take $\mu_{GB} = 100\mu_{BG} = 2.19 \times 10^9$ cm^3/g $\cdot$ day.

Sensitivity analysis

We performed sensitivity analysis with respect to the tumor volume at day 30 for the parameters λ_{DC}, $\lambda_{T_8 I_{12}}$, λ_{EG}, λ_{CW}, η_8, K_{TG}, ε_{DA}, μ_{CA}, μ_{GB} and K_{AB}, taking γ_A and γ_B as in Fig. 3(a) (but the same results hold for the choices of γ_A, γ_B as in Fig. 3(b) and Fig. 3(c)).

Following the method of [52], we performed Latin hypercube sampling and generated 5000 samples to calculate the partial rank correlation coefficients

(PRCC) and the p-values with respect to the tumor volume at day 30. In sampling all the parameters, we took the range of each parameter from 1/2 to twice its value in Table 2 and 3. The results are shown in Fig. 5.

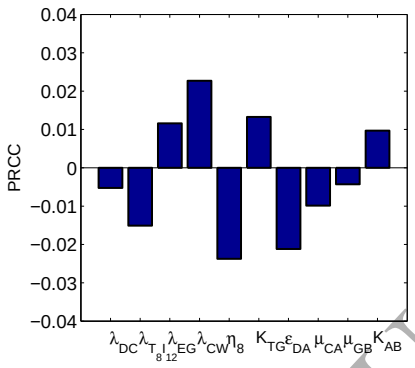

Figure 5: Statistically significant PRCC values (p-value< 0.01) for tumor volume at day 30; here $\gamma_A = 3 \times 10^{-9}$ g/cm$^3 \cdot$ day and $\gamma_B = 6 \times 10^{-9}$ g/cm$^3 \cdot$ day

.

From Fig. 5 we see that the rates η_8, by which CD8$^+$ T cells kill cancer cells, and $\lambda_{T_8 I_{12}}$, by which CD8$^+$ T cells are activated, are highly negatively correlated. The rate ε_{DA}, by which the chemotherapy induces activation of dendritic cells, and the rate μ_{CA}, by which chemotherapy kills directly cancer cells, are also highly negatively correlated. On the other hand, the growth rate of endothelial cells, λ_{EG}, and the oxygen-dependent growth rate of cancer cells, λ_{CW}, are positively correlated, as well as the blocking rate (K_{TG}) of T_8 by VEGF.

It is interesting to see that the rate, K_{AB}, by which anti-VEGF blocks the perfusion of the chemotherapy, is also positively correlated, i.e., when the blockade of the perfusion of chemotherapy is decreased (by B), the reduction of tumor volume by chemotherapy increases.

Computational method

We employ moving mesh method [32] to numerically solve the free boundary problem for the tumor proliferation model. To illustrate this method, we take Eq. (5) as example and rewrite it as the following form:

$$\frac{\partial C(r,t)}{\partial t} = \delta_C \Delta C(r,t) - div(\mathbf{u}C) + F, \tag{19}$$

where F represents the term in the right hand side of Eq. (5). Let r_i^k and C_i^k denote numerical approximations of i-th grid point and $C(r_i^k, n\tau)$, respectively, where τ is the size of time-step. The discretization of Eq. (19) is derived by the

fully implicit finite difference scheme:

$$\frac{C_i^{k+1}-C_i^k}{\tau}=\delta_C\left(C_{rr}+\frac{2}{r_i^k}C_r\right)-\left(\frac{2}{r_i^{k+1}}u_i^{k+1}+u_r\right)C_i^{k+1}-u_i^{k+1}C_r+F_i^{k+1}, \tag{20}$$

where $C_r=\frac{h_{-1}^2C_{i+1}^{k+1}-h_1^2C_{i-1}^{k+1}-(h_1^2-h_{-1}^2)C_i^{k+1}}{h_1(h_{-1}^2-h_1h_{-1})}$, $C_{rr}=2\frac{h_{-1}C_{i+1}^{k+1}-h_1C_{i-1}^{k+1}+(h_1-h_{-1})C_i^{k+1}}{h_1(h_1h_{-1}-h_{-1}^2)}$, $u_r=\frac{h_{-1}^2u_{i+1}^{k+1}-h_1^2u_{i-1}^{k+1}-(h_1^2-h_{-1}^2)u_i^{k+1}}{h_1(h_{-1}^2-h_1h_{-1})}$, $h_{-1}=r_{i-1}^{k+1}-r_i^{k+1}$ and $h_1=r_{i+1}^{k+1}-r_i^{k+1}$. The mesh moves by $r_i^{k+1}=r_i^k+u_i^{k+1}\tau$, where u_i^{k+1} is solved by the velocity equation.

Acknowledgements

This work is supported by the Mathematical Biosciences Institute and the National Science Foundation (DMS 0931642), and by the Renmin University of China and the National Natural Science Foundation of China (Grant No. 11501568), and the International Postdoctoral Exchange Fellowship Program 2016 by the Office of China Postdoctoral Council.

Author's contributions

AF and XL developed and simulated the model, and wrote the final manuscript. Both authors read and approved the final manuscript.

References

References

[1] D. Meulendijks, J. W. B. De Groot, M. Los, J. E. Boers, L. V. Beerepoot, M. B. Polee, A. Beeker, J. E. Portielje, S. H. Goey, R. S. De Jong, et al., Bevacizumab combined with docetaxel, oxaliplatin, and capecitabine, followed by maintenance with capecitabine and bevacizumab, as first-line treatment of patients with advanced her2-negative gastric cancer: A multicenter phase 2 study, Cancer 122 (9) (2016) 1434–1443.

[2] S. Delaloge, D. Pérol, C. Courtinard, E. Brain, B. Asselain, T. Bachelot, M. Debled, V. Dieras, M. Campone, C. Levy, et al., Paclitaxel plus bevacizumab or paclitaxel as first-line treatment for her2-negative metastatic breast cancer in a multicenter national observational study, Annals of Oncology 27 (9) (2016) 1725–1732.

[3] D. W. Miles, A. Chan, L. Y. Dirix, J. Cortés, X. Pivot, P. Tomczak, T. Delozier, J. H. Sohn, L. Provencher, F. Puglisi, et al., Phase iii study of bevacizumab plus docetaxel compared with placebo plus docetaxel for the

first-line treatment of human epidermal growth factor receptor 2–negative metastatic breast cancer, Journal of Clinical Oncology 28 (20) (2010) 3239–3247.

[4] H. Kim, K. Jung, S.-A. Im, Y.-H. Im, S. Kang, K. Park, S. Lee, S.-B. Kim, K.-H. Lee, J. Ahn, et al., Multicentre phase ii trial of bevacizumab combined with docetaxel–carboplatin for the neoadjuvant treatment of triple-negative breast cancer (kcsg br-0905), Annals of Oncology 24 (6) (2013) 1485–1490.

[5] D. Miles, C. Zielinski, M. Martin, E. Vrdoljak, N. Robert, Combining capecitabine and bevacizumab in metastatic breast cancer: a comprehensive review, European Journal of Cancer 48 (4) (2012) 482–491.

[6] L. Tiainen, M. Tanner, O. LAHDENPERÄ, P. Vihinen, A. Jukkola, P. Karihtala, N. Paunu, T. Huttunen, P.-L. Kellokumpu-Lehtinen, Bevacizumab combined with docetaxel or paclitaxel as first-line treatment of her2-negative metastatic breast cancer, Anticancer Research 36 (12) (2016) 6431–6438.

[7] K. Miller, M. Wang, J. Gralow, M. Dickler, M. Cobleigh, E. A. Perez, et al., Paclitaxel plus bevacizumab versus paclitaxel alone for metastatic breast cancer, N Engl J Med 357 (2007) 2666–2676.

[8] R. S. Turley, A. N. Fontanella, J. C. Padussis, H. Toshimitsu, Y. Tokuhisa, E. H. Cho, G. Hanna, G. M. Beasley, C. K. Augustine, M. W. Dewhirst, et al., Bevacizumab-induced alterations in vascular permeability and drug delivery: a novel approach to augment regional chemotherapy for in-transit melanoma, Clinical Cancer Research 18 (12) (2012) 3328–3339.

[9] C. V. Pastuskovas, E. E. Mundo, S. P. Williams, T. K. Nayak, J. Ho, S. Ulufatu, S. Clark, S. Ross, E. Cheng, K. Parsons-Reponte, et al., Effects of anti-vegf on pharmacokinetics, biodistribution, and tumor penetration of trastuzumab in a preclinical breast cancer model, Molecular Cancer Therapeutics 11 (3) (2012) 752–762.

[10] H. E. Daldrup-Link, Y. Okuhata, A. Wolfe, S. Srivastav, S. Øie, N. Ferrara, R. L. Cohen, D. M. Shames, R. C. Brasch, Decrease in tumor apparent permeability-surface area product to a mri macromolecular contrast medium following angiogenesis inhibition with correlations to cytotoxic drug accumulation, Microcirculation 11 (5) (2004) 387–396.

[11] M. Cesca, L. Morosi, A. Berndt, I. F. Nerini, R. Frapolli, P. Richter, A. Decio, O. Dirsch, E. Micotti, S. Giordano, et al., Bevacizumab-induced inhibition of angiogenesis promotes a more homogeneous intratumoral distribution of paclitaxel, improving the antitumor response, Molecular Cancer Therapeutics 15 (1) (2016) 125–135.

[12] S. Mollard, J. Ciccolini, D.-C. Imbs, R. El Cheikh, D. Barbolosi, S. Benzekry, Model driven optimization of antiangiogenics+ cytotoxics combination: application to breast cancer mice treated with bevacizumab+ paclitaxel doublet leads to reduced tumor growth and fewer metastasis, Oncotarget 8 (14) (2017) 23087–23098.

[13] M. R. Sharma, W. M. Stadler, M. J. Ratain, Randomized phase ii trials: a long-term investment with promising returns, Journal of the National Cancer Institute 103 (14) (2011) 1093–1100.

[14] M. L. Maitland, C. Hudoba, K. L. Snider, M. J. Ratain, Analysis of the yield of phase ii combination therapy trials in medical oncology, Clinical Cancer Research (2010) 1078–0432.

[15] G. P. Sims, D. C. Rowe, S. T. Rietdijk, R. Herbst, A. J. Coyle, Hmgb1 and rage in inflammation and cancer, Annu Rev Immunol 28 (2010) 367–388.

[16] L. Zandarashvili, D. Sahu, K. Lee, Y. S. Lee, P. Singh, K. Rajarathnam, et al., Real-time kinetics of high-mobility group box 1 (hmgb1) oxidation in extracellular fluids studied by in situ protein nmr spectroscopy, J Biol Chem 288 (17) (April 2013) 11621–11627.

[17] J. Palucka, J. Banchereau, Cancer immunotherapy via dendritic cells, Nat Rev Cancer 12 (4) (Mar 2012) 265–277.

[18] R. Saenz, D. Futalan, L. Leutenez, F. Eekhout, J. F. Fecteau, S. Sundelius, et al., Tlr4-dependent activation of dendritic cells by an hmgb1-derived peptide adjuvant, J Transl Med 12 (211) (Aug 2014) 1–11.

[19] C. Alfaro, N. Suarez, A. Gonzalez, S. Solano, L. Erro, J. Dubrot, A. Palazon, S. Hervas-Stubbs, A. Gurpide, J. M. Lopez-Picazo, et al., Influence of bevacizumab, sunitinib and sorafenib as single agents or in combination on the inhibitory effects of vegf on human dendritic cell differentiation from monocytes, British Journal of Cancer 100 (7) (2009) 1111–1119.

[20] D. I. Gabrilovich, H. L. Chen, K. R. Girgis, H. T. Cunningham, G. M. Meny, S. Nadaf, D. Kavanaugh, D. P. Carbone, Production of vascular endothelial growth factor by human tumors inhibits the functional maturation of dendritic cells, Nature medicine 2 (10) (1996) 1096–1103.

[21] J. M. T. Janco, P. Lamichhane, L. Karyampudi, K. L. Knutson, Tumor-infiltrating dendritic cells in cancer pathogenesis, J Immunol 194 (7) (Apr 2015) 2985–2991.

[22] Y. Ma, G. V. Shurin1, Z. Peiyuan, M. R. Shurin, Dendritic cells in the cancer microenvironment, J Cancer 4 (1) (2013) 36–44.

[23] J. E. Ohm, D. I. Gabrilovich, G. D. Sempowski, E. Kisseleva, K. S. Parman, S. Nadaf, D. P. Carbone, Vegf inhibits t-cell development and may contribute to tumor-induced immune suppression, Blood 101 (12) (2003) 4878–4886.

[24] J. K. Mulligan, S. A. Rosenzweig, M. R. I. Young, Tumor secretion of vegf induces endothelial cells to suppress t cell functions through the production of pge2, Journal of immunotherapy (Hagerstown, Md.: 1997) 33 (2) (2010) 126–135.

[25] N. G. Gavalas, M. Tsiatas, O. Tsitsilonis, E. Politi, K. Ioannou, A. C. Ziogas, A. Rodolakis, G. Vlahos, N. Thomakos, D. Haidopoulos, et al., Vegf directly suppresses activation of t cells from ascites secondary to ovarian cancer via vegf receptor type 2, British Journal of Cancer 107 (11) (2012) 1869–1875.

[26] A. C. Ziogas, N. G. Gavalas, M. Tsiatas, O. Tsitsilonis, E. Politi, E. Terpos, A. Rodolakis, G. Vlahos, N. Thomakos, D. Haidopoulos, et al., Vegf directly suppresses activation of t cells from ovarian cancer patients and healthy individuals via vegf receptor type 2, International journal of cancer 130 (4) (2012) 857–864.

[27] Y.-L. Li, H. Zhao, X.-B. Ren, Relationship of vegf/vegfr with immune and cancer cells: staggering or forward?, Cancer biology & medicine 13 (2) (2016) 206–214.

[28] B. Szomolay, T. D. Eubank, R. D. Roberts, C. B. Marsh, A. Friedman, Modeling the inhibition of breast cancer growth by gm-csf, J Theor Biol 303 (June 2012) 141–151.

[29] T. Chanmee, P. Ontong, K. Konno, N. Itano, Tumor-associated macrophages as major players in the tumor microenvironment, Cancers 6 (3) (Augest 2014) 1670–1690.

[30] W. Hao, A. Friedman, Serum upar as biomarker in breast cancer recurrence: A mathematical model, PLoS ONE 11 (4) (Apr 2016) e0153508.

[31] D. Chen, J. M. Roda, C. B. Marsh, T. D. Eubank, A. Friedman, Hypoxia inducible factors-mediated inhibition of cancer by gm-csf: a mathematical model, Bulletin of mathematical biology 74 (11) (2012) 2752–2777.

[32] B. D'Acunto, Computational Methods for PDE in mechanics, Series on Advances in Mathematics for Applied Sciences-Vol.67, Word Scientific, Singapore, 2004.

[33] L. D. Volk, M. J. Flister, C. M. Bivens, A. Stutzman, N. Desai, V. Trieu, et al., Nab-paclitaxel efficacy in the orthotopic model of human breast cancer is significantly enhanced by concurrent anti-vascular endothelial growth factor a therapy, Neoplasia 10 (6) (2008) 613–623.

[34] Q. Zhang, V. Bindokas, J. Shen, H. Fan, R. M. Hoffman, H. R. Xing, Time-course imaging of therapeutic functional tumor vascular normalization by antiangiogenic agents, Mol Cancer Ther 10 (7) (July 2011) 1173–1184.

[35] E. Guerin, S. Man, P. Xu, R. S. Kerbel, A model of postsurgical advanced metastatic breast cancer more accurately replicates the clinical efficacy of antiangiogenic drugs, Cancer Res 73 (9) (May 2013) 2743–2748.

[36] D. Miles, G. von Minckwitz, A. D. Seidman, Combination versus sequential single-agent therapy in metastatic breast cancer, The Oncologist 7 (Supplement 6) (2002) 13–19.

[37] K. Fujimoto-Ouchi, Y. Tanaka, T. Tominaga, Schedule dependency of antitumor activity in combination therapy with capecitabine/5?-deoxy-5-fluorouridine and docetaxel in breast cancer models, Clinical Cancer Research 7 (4) (2001) 1079–1086.

[38] E. Frei III, J. P. Eder, Principles of dose, schedule, and combination therapy, Cancer Medicine 7 (2003) 590–599.

[39] G. Cabibbo, S. Tremosini, G. Galati, G. Mazza, G. Gadaleta-Caldarola, G. Lombardi, M. Antonucci, R. Sacco, Transarterial chemoembolization and sorafenib in hepatocellular carcinoma, Expert review of anticancer therapy 14 (7) (2014) 831–845.

[40] A. Friedman, W. Hao, The role of exosomes in pancreatic cancer microenvironment, Bulletin of Mathematical Biology (2017) 1–23.

[41] X. Lai, A. Friedman, Combination therapy of cancer with braf inhibitor and immune checkpoint inhibitor: A mathematical model, BMC System Biology 11 (70) (2017) 1–18. doi:DOI10.1186/s12918-017-0446-9.

[42] K. L. Liao, X. F. Bai, A. Friedman, Mathematical modeling of interleukin-27 induction of anti-tumor t cells response, PLoS ONE 9 (3) (2014) e91844.

[43] Y. Kim, S. Lawler, M. O. Nowicki, E. A. Chiocca, A. Friedman, A mathematical model for pattern formation of glioma cells outside the tumor spheroid core, J Theor Biol 260 (3) (Oct 2009) 359–371.

[44] Y. Kim, J. Wallace, F. Li, M. Ostrowski, A. Friedman, Transformed epithelial cells and fibroblasts/myofibroblasts interaction in breast tumor: a mathematical model and experiments., J Theor Biol 61 (3) (Sep 2010) 401–421.

[45] M. E. Young, Estimation of diffusion coefficients of proteins, Biotechnology and Bioengineering XXII (1980) 947–955.

[46] Y. B. Shui, X. Wang, J. S. Hu, S. P. Wang, C. M. Garcia, et al., Vascular endothelial growth factor expression and signaling in the lens, Invest Ophthalmol Vis Sci 44 (9) (2003) 3911–3919.

[47] T. Hamza, J. B. Barnett, B. Li, Interleukin 12 a key immunoregulatory cytokine in infection applications, Int J Mol Sci 11 (3) (Feb 2010) 789–806.

[48] C. Androjna, J. E. Gatica, J. M. Belovich, K. A. Derwin, Oxygen diffusion through natural extracellular matrices: implications for estimating "critical thickness" values in tendon tissue engineering, Tissue Engineering Part A 14 (4) (2008) 559–569.

[49] D. Chen, A. A. Bobko, A. C. Gross, R. Evans, C. B. Marsh, V. V. Khramtsov, et al., Involvement of tumor macrophage hifs in chemotherapy effectiveness: mathematical modeling of oxygen, ph, and glutathione, PLoS ONE 9 (10) (Oct 2014) e107511.

[50] Y.-W. Lim, B.-C. Goh, L.-Z. Wang, S.-H. Tan, B. Y. S. Chuah, S.-E. Lim, et al., Pharmacokinetics and pharmacodynamics of docetaxel with or without ketoconazole modulation in chemonaive breast cancer patients, Annals of Oncology 21 (11) (April 2010) 2175–2182.

[51] S. Agrawal, M. Joshi, J. B. Christoforidis, Vitreous inflammation associated with intravitreal anti-vegf pharmacotherapy, Mediators of inflammation 2013 (943409) (2013) 1–6.

[52] S. Marino, I. Hogue, C. Ray, D. Kirschner, A methodology for performing global uncertainty and sensitivity analysis in systems biology, J Theor Biol 254 (1) (2008) 178–196.